4H-SiC UV photo detectors with large area and very high specific detectivity

Feng Yan, *MEMBER, IEEE*, Xiaobin Xin, Shahid Aslam,

Yuegang Zhao, *MEMBER, IEEE* , David Franz, Jian H. Zhao, *SENIOR MEMBER, IEEE*,

and Maurice Weiner, *FELLOW, IEEE.*

Abstract Pt/4H-SiC Schottky photodiodes have been fabricated with the device areas up to $1cm^2$. The *I-V* characteristics and photo-response spectra have been measured and analyzed. For a 5mm×5mm area device leakage current of 1×10^{-15}A at zero bias and 1.2×10^{-14}A at –1V have been established. The quantum efficiency is over 30% from 240nm to 320nm. The specific detectivity, D^*, has been calculated from the directly measured leakage current and quantum efficiency data and are shown to be higher than $10^{15}cmHz^{1/2}/W$ from 210nm to 350nm with a peak D^* of 3.6×10^{15} $cmHz^{1/2}/W$ at 300nm.

Index terms: ultraviolet detectors, Schottky diodes, detectors, photodiode, and leakage current

Footnote: The work at NASA Goddard Space Flight Center was partially supported by the U.S. Department of Commerce, NOAA/E/OSD (Ref. No: NE-EK0000-2-00302).

Contact Person:

Feng Yan

Tel: 301-286-7012

Fax: 301-286-1672

Email: fyan@pop500.gsfc.nasa.gov

Address: NASA-GSFC, Bldg. 11/Rm. E017, Greenbelt Road, Greenbelt, MD 20771

Affiliation of authors

Feng Yan, Aslam Shahid, and David Franz are with Raytheon/NASA-Goddard Space Flight Center, Greenbelt Road, Greenbelt, MD20771.

Xiaobin Xin and Jian H. Zhao are with Dept. of ECE, Rutgers University, 94 Brett Road, Piscataway, NJ28054

Yuegang Zhao is with Keithley Instruments, Inc., 30500 Bainbridge Road, Cleveland, OH 44139-2216

Maurice Weiner is with United Silicon Carbide, Inc., 100 Jersey Ave, New Brunswick, NJ08901

I. INTRODUCTION

The sensitivity of a photo-detector is primarily limited by the background radiation (e.g. the 300K blackbody radiation of the earth) and the noise of the detector, which increases as the leakage current increases [1]. Since the 300K blackbody radiation is mainly in the visible and infrared range, it limits the sensitivity of most photo-detectors that have cut-off's in this range but barely affects those detectors with cut-off's in the ultra-violet (UV) range, *i.e.* the visible blind photo-detectors. The solar radiation is practically zero on the earth in the solar blind UV range from 245nm and 280nm [2]. The photo-detection in this range is not affected by the solar radiation and is practically solar blind. Therefore, if photo-detectors can be fabricated with high quantum efficiency, low leakage current, and visible blindness or even solar blindness, photo-detection with very high sensitivity can be achieved even under solar irradiation background. In practice, high sensitivity visible blind or solar blind UV detectors are highly sought after for astronomical and terrestrial applications.

In the past decade, tremendous progress has been made in the material growth and processing of wide bandgap semiconductors, particularly SiC and GaN, and high quality SiC and GaN wafers are now commercially available [3],[4]. Both types of semiconductors have very wide bandgap (4H-SiC=3.2eV and GaN=3.4eV) and are visible blind. Due to the wide bandgap of SiC and GaN, the leakage current can be many orders of magnitude lower than the leakage current of Si detectors, making SiC and GaN good candidates for high sensitivity visible blind UV detection.

Compared with GaN, SiC has much better material maturity. For example, the defect density of SiC, $10\sim10^3/cm^3$ [5], is many orders of magnitude lower than that of GaN,

10^6~10^{10}/cm^3 [4]. Additionally, SiC substrate and epi-growth technology has developed to such a level as to allow the fabrication of many different types of SiC photo-detectors with desired features. Furthermore, 4H-SiC has very high breakdown field, outstanding radiation hardness, excellent chemical and mechanical rigidity, good thermal conductivity and as such are excellent candidates for photo detection in high temperature and high radiation environment conditions[3], [6]. SiC UV *pin* photodiodes have already been fabricated [7] and are commercially available. SiC avalanche photodiodes with extremely high gain (10^7) and low excess noise have also been demonstrated [8],[9]. In this paper we report on the fabrication of 4H-SiC Schottky photodiodes with large areas (up to 1cm×1cm) which show extremely low leakage current and excellent detectivity in the UV range.

II. DEVICE FABRICATION

4H-SiC Schottky photodiodes are fabricated on 2' production grade 4H-SiC wafers purchased from Cree, Inc., which have an n^- epilayer grown on n^+ substrate. The wafers were first oxidized in wet oxygen at 1050°C for 3 hours. Another 200nm PECVD SiO_2 and 300nm PECVD Si_3N_4 were then deposited on the top of the n^- side as the passivation layer. After oxide removal from the backside of the wafer, Ni was deposited on the n^+ side for *n*-type ohmic contact. The *n*-type ohmic contact was formed by annealing samples at 1050°C for 10 minutes in the N_2 forming gas with 3.5% H_2. After oxide etching, 75Å semi-transparent Pt was deposited on n^- side to form Schottky contact. A gold contact ring for wire bonding was then deposited on the top of the semi-transparent Pt. The width of the contact ring is 100μm. 4H-SiC Schottky diodes of four different

sizes have been fabricated and the areas are 0.25mm×0.50mm, 2mm×2mm, 5mm×5mm, and 1cm×1cm, respectively. Figure 1a) and b) shows the top view and the cross sectional view of the 4H-SiC Schottky photodiodes fabricated.

III. RESULTS

A. *Doping profile*

CV measurements were taken by Keithley 590 *CV* analyzer to determine the doping profile. The measurement was carried out at 100KHz. Figure 2 shows the corresponding doping profile determined from $d(1/C^2)/dV$. As shown in Fig. 2, the thickness of the n^- layer is about 3.7μm and the doping concentration varies from $3\times10^{14}/cm^3$ at the surface to $3\times10^{15}/cm^3$ at the interface between n^- epi-layer and substrate.

B. *IV measurement*

I-V characteristics of Pt/SiC Schottky diodes are measured by Keithley 4200 semiconductor characterization system at room temperature in the dark. Figure 3 shows the typical I-V characteristics of diodes of different sizes. The forward current of semi-log *I-V* shows excellent linearity across nine orders of magnitude. For metal/semiconductor Schottky diodes, the current can be expressed by [10]

$$I = A \cdot A^* \cdot T^2 \cdot \exp\left(-\frac{q\Phi_b}{nk_BT}\right) \cdot \left[\exp\left(\frac{qV}{nk_BT}\right) - 1\right], \qquad (1)$$

according to the thermoionic emission theory, where A is the area of the diode, A^* is Richardson's constant, Φ_b is the barrier height, n is the ideality factor, k_B is Boltzmann's constant, q is the electron charge, and T is the absolute temperature. Using the theoretical

Richardson's constant, 146A/W [11], the ideality factor and the Schottky barrier height were determined by fitting the linear region of the forward *I-V* curves.

Figure 4 summarizes the ideality factor and barrier height of diodes of different sizes. The ideality factor is around 1.05 for all other diodes except for the 1cm × 1cm diode, which showed an ideality factor of 1.20. The average barrier height of the 5mm×5mm diodes determined from *IV* characteristics is 1.52eV.

According to the relationship given by Itoh *et al* [11], the barrier height of 4H-SiC Schottky contact can be expressed by

$$\Phi_b = 0.70 \cdot \Phi_m - 1.95, \qquad (2)$$

where Φ_m is the work function of the Schottky metal. By using the 5.65eV work function of Pt, the barrier height of Pt/4H-SiC Schottky junction is 2.0eV, which is substantially higher than the barrier height determined from *IV* measurement results. The difference is still under investigation and is partially attributed to the inhomogeneous barrier height effect [12], [13]. It is also noted that the barrier height decreases as the area of the photodiode increases. Therefore, macro-defects, such as micropipes and polytype inclusions (density<10/cm^2), are likely to be responsible for the lowering of barrier height, too.

As shown in Fig.3, the leakage current is around 10^{-13}A between 0 and -1V for all diodes. The leakage current of all diodes except for the 1cm × 1cm one remains well below 10^{-12} A up to -5V. The results are very reproducible from batch to batch. Three 5mm×5mm, three 2mm×2mm, and one 1cm×1cm diodes have been fabricated in four different batches. All of them showed very consistent results. The measured leakage current does not show any area dependence and seems limited by the background noise. In order to

determine the actual leakage current, one 5mm×5mm diode was tested with calibrated equipment at the laboratories of Keithley, Inc.

The leakage current was measured at Keithley with a Keithley 4200 and pre-amplifier remotely mounted on to probe station to minimize any cable leakage. The measurement was carried out in a light–proof Cascade Summit 12000 testing system. Since the capacitance of the diode is relatively large (~5nF), the measured current is the combination of leakage current and the displacement current due to voltage ramp. Figure 5 shows the leakage current measured between 0 and -1V with the settling time was long enough to make the displacement current negligible. The diode shows the leakage current lower than 1fA at 0V, which is under the noise floor of the measurement instrument, and 12fA at -1V. The corresponding leakage current density is <4fA/cm^2 at 0V and 50fA/cm^2 at -1V. Note that the leakage current density of Pt/SiC Schottky diodes at room temperature is now comparable to the leakage current of photo-cathodes [14]. The dynamic resistance, R_o, at 0V is determined from $(dV/dI)_{V=0}$ to be $1\times10^{14}\Omega$ for the 5mm×5mm diode. The corresponding R_oA is $2.5\times10^{13}\Omega cm^2$.

The directly measured leakage current at zero bias is many orders of magnitude higher than the saturation current determined from forward *I-V* curves, which is typically around 10^{-20}A for 5mm×5mm diodes. The difference can be explained in two ways. One is that the leakage current is dominated by the different mechanisms at low bias voltage and the real leakage current is higher than the saturation current. The other is that the measured leakage current is from the noise of the device under test and the testing system. If so, the calculated R_o represents the lower-bound of the dynamic resistance. The actual R_o is likely to be higher.

C. Photo-response measurement

The quantum efficiency of the SiC Schottky photodiodes has been determined based on the photo-response spectra between 200nm and 400nm, which is shown in Fig. 6. 4H-SiC is indirect semiconductor with a bandgap of 3.2eV. Unlike GaN detectors, which have a sharp cut-off edge at the band edge, the quantum efficiency of 4H-SiC Shcottky diodes increases gradually from less than 0.1% at 380nm to 37% at 300nm. The maximum quantum efficiency is around 37% and nearly constant from 240nm to 300nm. The absorption coefficient of Pt at 300nm is 9.2×10^5 [15] and the semitransparent 75Å Pt will absorb 50% of the photons at 300nm. Therefore, the internal quantum efficiency is about 80% even without including the reflection loss. At wavelengths shorter than 240nm, the quantum efficiency decreases as the wavelength decreases. This decrease is most likely due to the influence of the surface recombination, which becomes significant when the penetration depth starts to be comparable with the dead zone caused by the surface recombination.

The uniformity of the quantum efficiency has also been checked across a 5mm×5mm device. The fluctuation of the quantum efficiency is 9% across the device. The average quantum efficiency in the center is about the same as the quantum efficiency at the edge, indicating that the photo-generated carriers can be efficiently collected by the 75Å Pt thin film.

For a detector at zero bias, the noise of the detector is dominated by the Johnson noise. D^* is one of the most frequently used figure of merits to evaluate the sensitivity of photo-detectors and is defined as [16],

$$D^* = \frac{q\eta}{h\nu} \cdot \left[\frac{R_o A}{4k_B T} \right]^{1/2}, \qquad (3)$$

when the Johnson noise dominates, where η is the quantum efficiency, h is the Planck constant, ν is the radiation frequency, R_o is the dynamic resistance at zero bias, and A is the detector area. The D^* of 4H-SiC Schottky photodiodes is calculated based on the directly measured results of our 5mm×5mm photodiodes and compared with other common photo detectors in Fig. 7. The maximum D^* of 4H-SiC Schottky is 3.6×10^{15} $cmHz^{1/2}/W$ at 300nm and the D^* is above 10^{15} $cmHz^{1/2}/W$ from 210nm to 350nm. The D^* is two orders of magnitude higher than the D^* of Si photodiodes, and three orders of magnitude higher than the D^* of Si CCD [14] [17]. As expected, the D^* of SiC photodiodes is not limited by the 300K background limit, or the D^* of background limited infrared photodiodes (BLIP), as most infrared detectors.

The D^* of SiC Schottky photodiodes is still about one order of magnitude lower than S20 PMT. It should be noted that the current results are achieved on SiC wafers containing many types of surface defects [5], which will cause inhomogeneous barrier height across the devices. As a result, the effective barrier height is substantially lower than the ideal value, 2.0eV for Pt/4H-SiC. As the SiC crystal quality improves, giving rise to low surface defects density, the barrier height can be substantially increased and the leakage current can be further reduced even for large area photodiodes. Moreover, the quantum efficiency can be further improved by reducing the thickness of the semitransparent metal. Therefore, it should be possible to fabricate SiC photodiodes with D^* higher than or at least comparable to most PMTs.

It should also be pointed out that the demonstrated SiC photodiodes show good quantum efficiency across the solar blind UV, 245nm to 280nm even though the top Pt film absorb 50% of incident photons. For small area detectors which do not require continuous Pt film to collect the photon generated holes, quantum efficiency higher than 80% should be achievable. Considering the harsh requirement of solar blind detection, a cut-off rate of 10dB/nm from 285 to 300nm, solar blind detection may be practically unachievable for semiconductor detectors without special filters [2], [18]. The high D* SiC photodiodes reported here, although not intrinsically solar blind, are however very good candidates for solar blind UV detection when employed with proper solar blind filters.

IV. CONCLUSION

Pt/4H-SiC Schottky photodiodes with the device area of 0.25mm×0.50mm, 2mm×2mm, 5mm×5mm, and 1cm×1cm have been fabricated and characterized. The *I-V* measurement results show that the ideality factor is less than 1.05 for diodes up to 5mm×5mm. The photodiodes showed extremely low leakage current. The leakage current of a 5mm×5mm device is less than 1×10^{-15}A at zero bias and 1.2×10^{-14}A at -1V. The photo-response results show that the quantum efficiency is over 30% and nearly flat from 320nm to 240nm. The D^* at zero bias has been calculated based on the directly measured dynamic resistance at zero bias. The peak of the D^* of 4H-SiC Schottky is found to be 3.6×10^{15} cmHz$^{1/2}$/W at 300nm and the D^* is above 10^{15} cmHz$^{1/2}$/W from 210nm to 350nm.

ACKNOWLEDGEMENT: The author, Feng Yan, likes to thank Dr. Carl Stahle of Goddard Space Flight Center and Dr. Charles Joseph of Dept. of Physics at Rutgers University for the support and helpful discussion on this work.

REFERENCES

[1] P. W. Kruse, "The photo detection process" in *Optical and Infrared Detectors*, New York: Springer-Verlag, 1977, pp. 5-69.

[2]. R.E. Huffman, "Atmospheric emission and absorption of ultraviolet radiation" in *Handbook of Geophysics and the Space Environment*, A. S. Jursa Ed., Air Force Geophysics Laboratory, 1985, pp.22.1-22.7.

[3]. A. R. Powell and L. B. Rowland, "SiC Materials-Progress, Status, and Potential Roadblocks", *Proc. IEEE*, vol. 90, pp. 942-955, Jun., 2002.

[4]. M. Razeghi, "Short-wavelength solar blind detectors-status, prospects, and markets", *Proc. IEEE*, vol. 90, pp. 1006-1014, Jun., 2002.

[5]. P. G. Neudeck, "Electrical impact of SiC structural crystal defects on high field devices", *Material Science Forum* vol. 338-342, pp. 1161-1166, Oct., 2000.

[6]. A. L.Barry, B. Lehmann, D. Fritsch, and D. Braunig, "Energy dependence of electron damage and displacement threshold energy in 6H-SiC", *IEEE Trans. Nucl. Sci.*, vol. 38, pp. 1111-1115, Jun., 1991.

[7]. J. A. Edmond, H. Kong, and C. H. Carter Jr., "Blue LEDs, UV photodiodes and high temperature rectifier in 6H-SiC", *Physica B: Condensed Matter,* vol. 185, pp. 453-460, Apr. 1993.

[8]. F. Yan, C. Qin, J. H. Zhao, M. Weiner, B. K. Ng, J. P. R. David, R. C. Tozer, "Low-noise visible-blind UV avalanche photodiodes with edge terminated by 2 degrees positive bevel", *Electronics Lett.*, vol. 38, pp. 335-336, Jul., 2002.

[9]. X. Guo, A. Beck, B. Yang, and J.C. Campbell, "Low dark current 4H-SiC avalanche photodiodes", *IEEE Electronics Lett.,* vol. 39, pp. 1673-1674, Nov. 2003.

[10]. E. H. Rhoderick and R. H. Williams, "Metal semiconductor contact", 2nd Ed., Oxford: Clarebdon Press, 1978, pp. 46-47.

[11]. A. Itoh, and H. Matsunami, "Analysis of Schottky Barrier Heights of Metal/SiC Contacts and Its Possible Application to High-Voltage Rectifying Devices", *phys.stat. sol. (a)* vol. 162, pp. 389-408, Jul, 1997.

[12]. R. T. Tung, "Electron transport at metal-semiconductor interfaces: general theory", *Phys. Rev. B*, vol. 45, 13509-13523, Jun., 1992.

[13]. F. Roccaforte, F. L. Via, V. Raineri, R. Pierobon, and E. Zanoni, "Richardson's constant in inhomogeneous silicon carbide Schottky contacts", *J. Appl. Phys.*, vol. 93, pp. 9137-9144, Jun., 2003.

[14]. S. Donati, "Photo-detectors-devices, circuits, and applications", New Jersey: Prentice Hall, 2000, pp. 1-46.

[15]. E. D. Palik, "Optical constants of materials", San Diego: Academic Press, 1985, pp. 333-341.

[16]. S. L. Chuang, "Physics of optoelectronic devices", New York: John Wiley & Sons, 1995, pp. 583-630.

[17]. *The Book of Photon Tools*, Stratford: Oriel Instruments, pp. 6.1-6.140.

[18]. S. Verghese, K. A. McIntosh, R. J. Molnar, L. J. Mahoney, R. L. Aggarwal, M. W. Geis, K. M. Molvar, E. K. Duerr,, and I. Melngailis, "GaN photodiodes operating in linear gain mode and Geiger mode", *IEEE Trans. Electron Devices*, vol. ED-48, pp. 502-511, Mar., 2001.

FIGURE CAPTIONS

Figure 1 a). The top view of a 1cm×1cm Pt/4H-SiC Schottky photodiode and b). the cross-sectional view of Pt/4H-SiC Schottky photodiodes

Figure 2 The doping profile of 4H-SiC wafers determined from CV measurement at 100KHz

Figure 3 Typical I-V characteristics of Pt/4H-SiC Schottky photodiodes of different sizes from 0.25mm×0.5mm to 1cm×1cm

Figure 4 The barrier heights and ideality factors of Pt/4H-SiC Schottky photodiodes of different sizes determined from their forward I-V characteristics

Figure 5 Reverse I-V characteristics of a 5mm×5mm Pt/4H-SiC Schottky photodiode

Figure 6 Typical photo response spectra in quantum efficiency of Pt/4H-SiC Schottky photodiodes

Figure 7 The comparison between SiC Schottky 5mm×5mm photodiodes made in this work and some common detectors [13], [16]. The 300K blackbody radiation limited D^* (300K BLIP) is also inset as a reference.

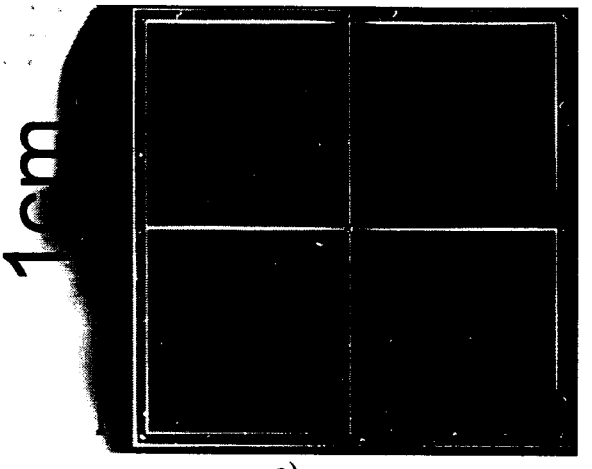

a)

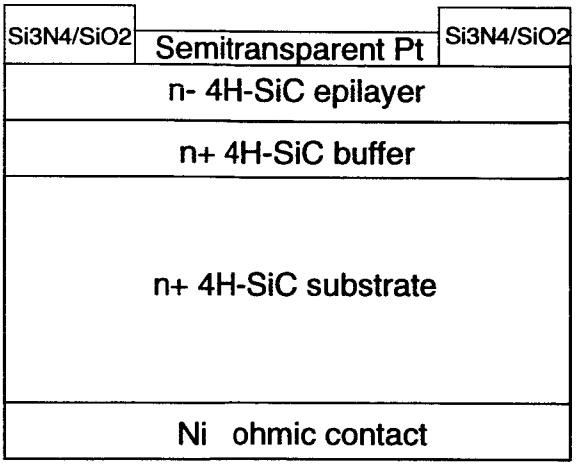

b)

Figure 1. a) The top view of a 1cm×1cm Pt/4H-SiC Schottky photodiode and b) the cross-sectional view of Pt/4H-SiC Schottky photodiodes.

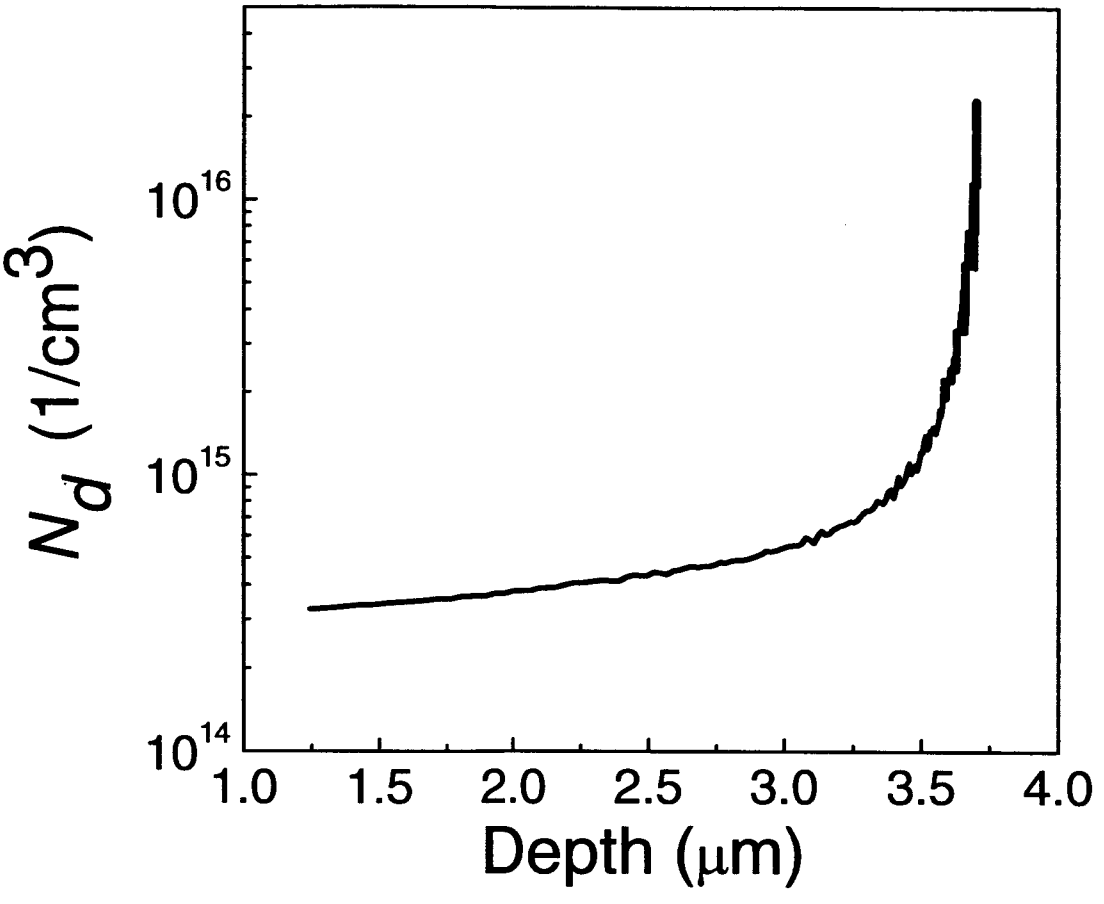

Figure 2 The doping profile of 4H-SiC wafers determined from CV measurement at 100K Hz

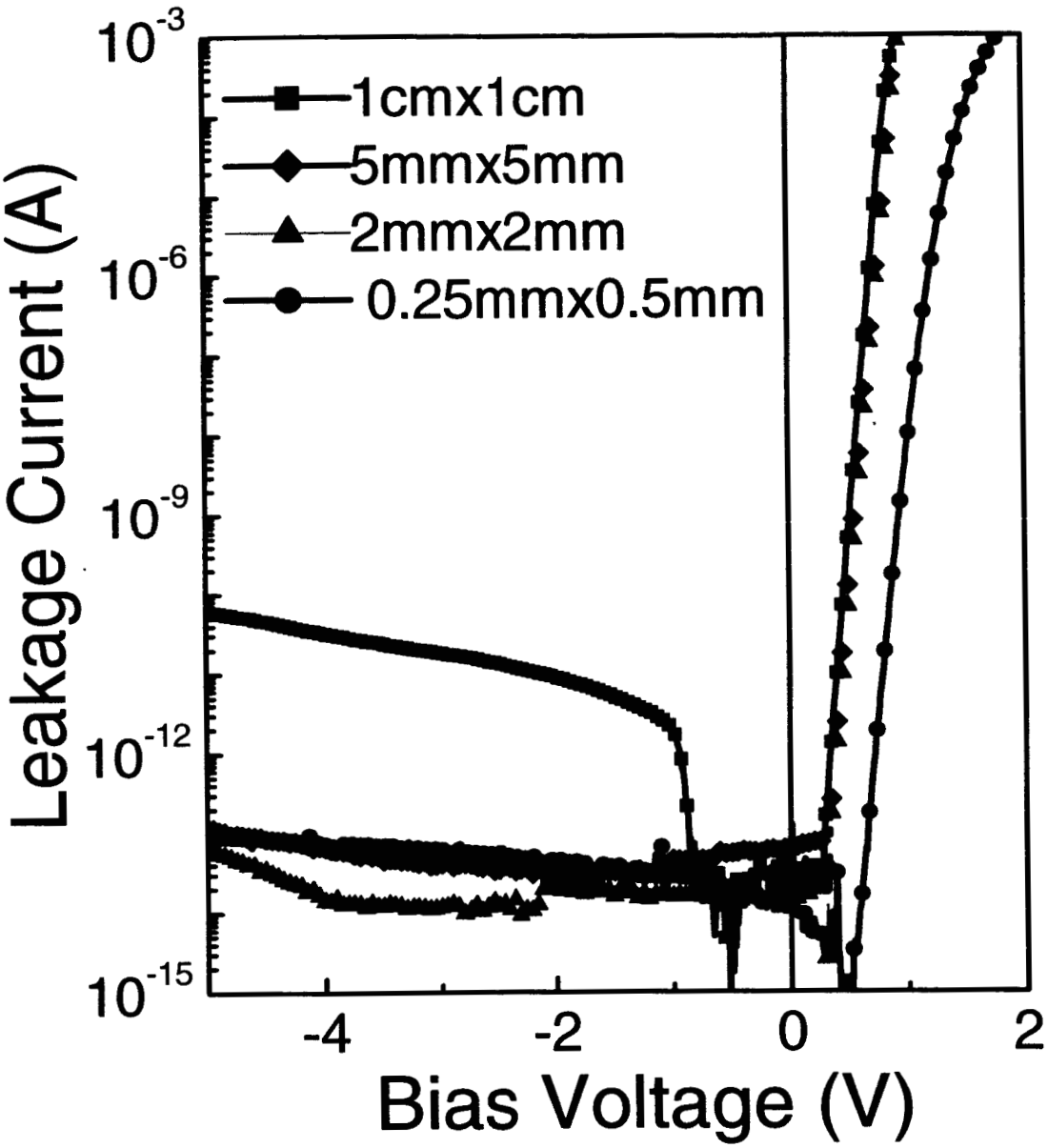

Figure 3. Typical I-V characteristics of Pt/4H-SiC Schottky photodiodes of different sizes from 0.25mm×0.5mm to 1cm×1cm

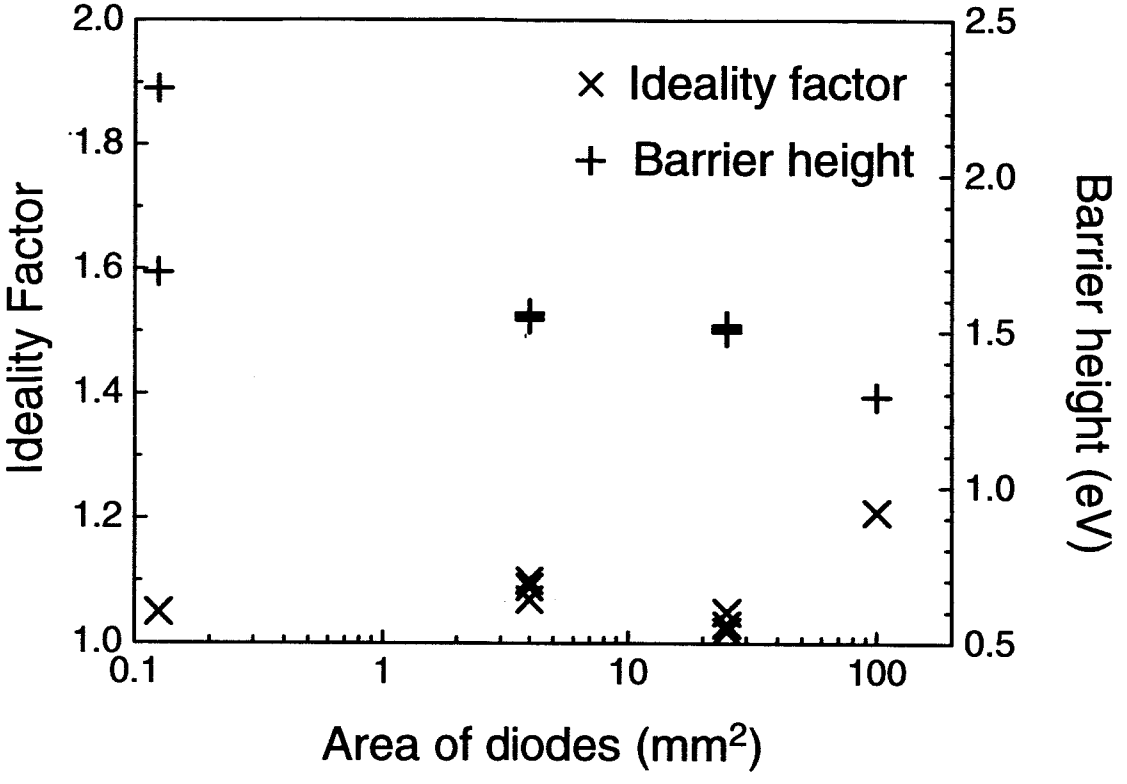

Figure 4. The barrier heights and ideality factors of Pt/4H-SiC Schottky photodiodes of different sizes determined from their forward I-V characteristics

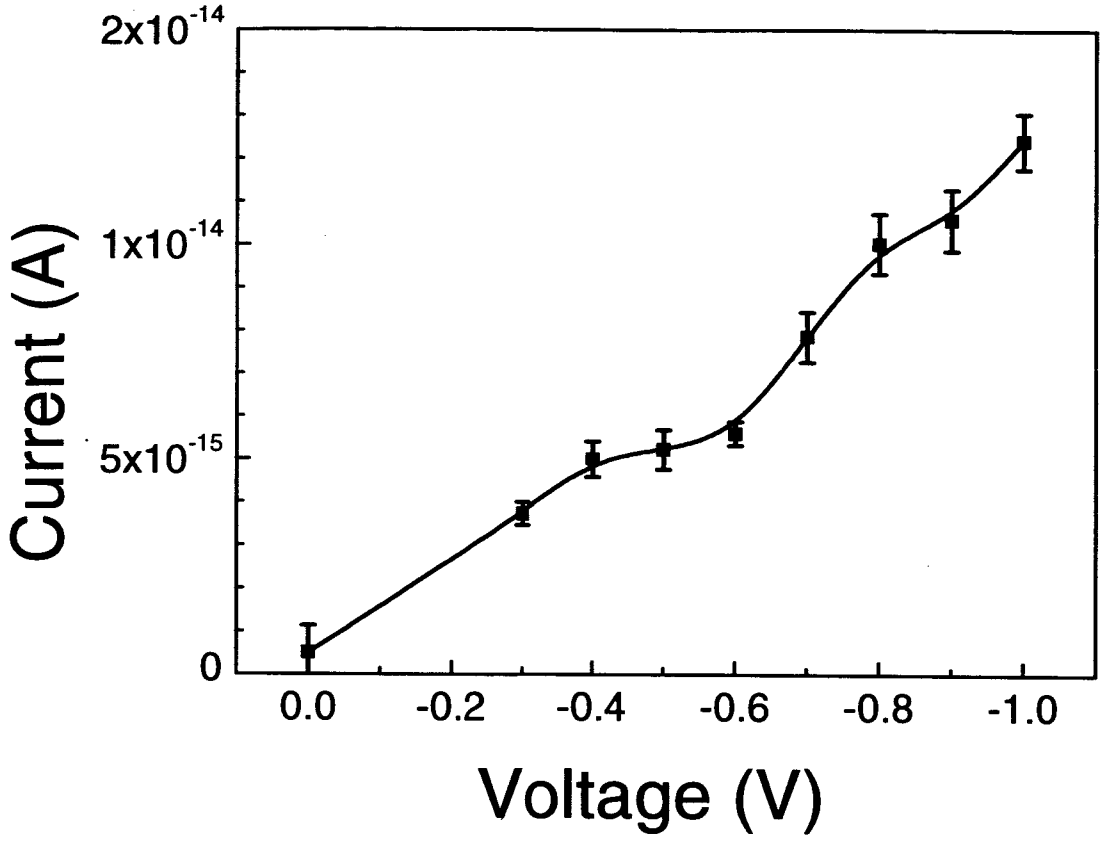

Figure 5. Reverse I-V characteristics of a 5mm×5mm Pt/4H-SiC Schottky photodiode

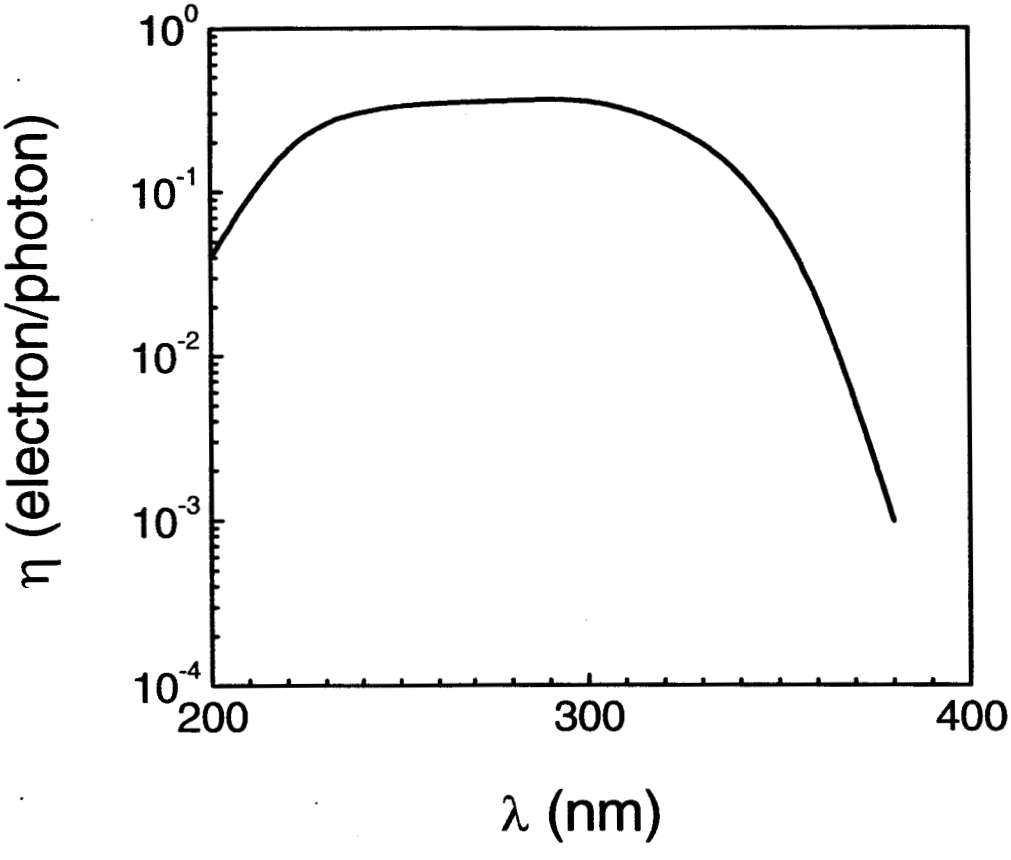

Figure 6. The photo response spectra in quantum efficiency of Pt/4H-SiC Schottky photodiodes

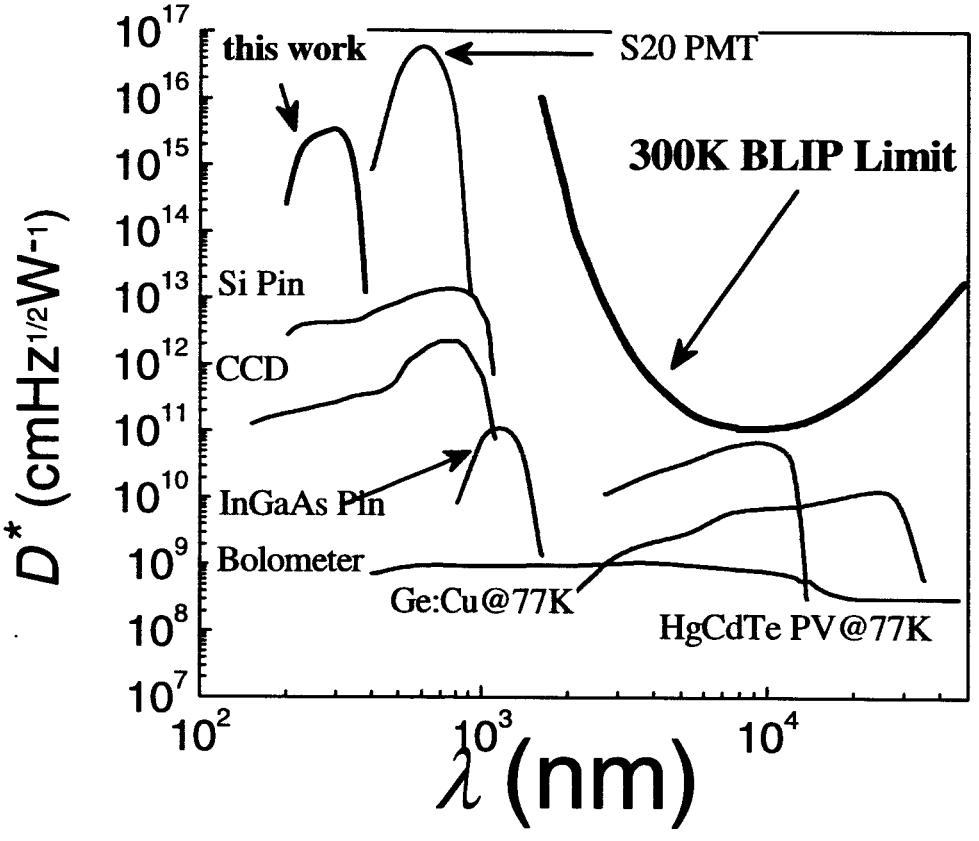

Figure 7 The comparison between SiC Schottky 5mm×5mm photodiodes made in this work and some common detectors [14], [17]. The 300K blackbody radiation limited D^*, 300K BLIP limit, is also inset as a reference.